

## Neutrino luminosity of stars with different masses

Yang Shi<sup>1</sup>, Xun Xue<sup>1,2</sup>, Chun-Hua Zhu<sup>1</sup>, Zhao-Jun Wang<sup>1</sup>, He-Lei Liu<sup>1</sup>, Lin Li<sup>1</sup> and Guo-Liang Lü<sup>1</sup>

<sup>1</sup> School of Physics and Technology, Xinjiang University, Urumqi 830046, China; [sy4289208@163.com](mailto:sy4289208@163.com)

<sup>2</sup> Department of Physics, East China Normal University, Shanghai 2000062, China

Received 2019 March 2; accepted 2019 July 23

**Abstract** Neutrinos play an important role in stellar evolution. They are produced by nuclear reactions or thermal processes. Using the stellar evolution code Modules for Experiments in Stellar Astrophysics (MESA), we study stellar neutrino luminosity with different masses. The neutrino luminosities of stars with different initial masses at different evolutionary stages are simulated. We find that the neutrino flux of a star with  $1 M_{\odot}$  mass at an evolutionary age of  $4.61 \times 10^9$  yr is consistent with that of the Sun. In general, neutrinos are produced by nuclear reactions, and the neutrino luminosity of stars is about one or two magnitudes lower than the photo luminosity. However, neutrino luminosity can exceed photo luminosity during the helium flash which can occur for stars with a mass lower than  $8 M_{\odot}$ . Although the helium flash does not produce neutrinos, plasma decay, one of the thermal processes, can efficiently make neutrinos during this stage. Due to the high mass-loss rate, a star with a mass of  $9 M_{\odot}$  does not undergo the helium flash. Its neutrinos mainly originate from nuclear reactions until the end of the AGB stage. At the end of the AGB stage, its neutrino luminosity results from plasma decay which is triggered by the gravitational energy release because of the stellar core contracting.

**Key words:** stars: evolution — stars: fundamental parameters — nuclear reactions — nucleosynthesis — abundances

### 1 INTRODUCTION

Neutrinos play an important role in astrophysics. Because they participate in weak interaction, they can escape freely (Raffelt 2012) and carry information from the stellar interior (Gamow & Schoenberg 1941). In addition, neutrinos have very strong penetrative force and very small cross section, which makes all stars transparent to their radiation (Masevich et al. 1965). Studying the properties of neutrinos has been one of the most exciting and vigorous activities in particle physics and astrophysics ever since Pauli first proposed their existence in 1930. There are several neutrino detectors currently in operation in the world. Baikal, ANTARES and IceCube have made great progress in detecting high-energy neutrinos. Recently, IceCube found that high-energy neutrinos may be emitted by the blazar TXS 0506+056 (IceCube Collaboration et al. 2018). Homestake, Kamiokande, GALLEX/GNO, SAGE and Super-Kamiokande have made a great contribution to our understanding of neutrino physics via observing solar neutrinos. In particular, Homestake and Kamiokande de-

tected the neutrinos emitted by supernova 1987A (Bionta et al. 1987; Hirata et al. 1987).

To some extent, stars are the most realistic representatives of neutrinos. Based on Weinberg-Salam theory, the neutrinos emitted from a star are produced by nuclear reactions or recombination processes which include plasmon decay, pair annihilation, bremsstrahlung, recombination, and photo-neutrinos (e.g., Itoh & Kohyama 1983; Kohyama et al. 1993; Itoh et al. 1996). The latter are also known as thermal processes (e.g., Bhattacharyya 2006; Paxton et al. 2013). However, most works focus on solar or supernova neutrinos (e.g., Bahcall & Ulrich 1988; Bahcall et al. 2001; Keil et al. 2003; Sukhbold et al. 2016). However, the neutrinos produced by stars with different masses and at different evolutionary stages are seldom investigated.

In this paper, we focus on the change in neutrino luminosities with stellar evolution, and compare them with photo luminosity. In Section 2, we present our assumptions and describe some details of the modeling algorithm.

In Section 3, we present a detailed evolution for neutrino luminosity. Conclusions follow in Section 4.

## 2 MODEL

Modules for Experiments in Stellar Astrophysics (MESA) is an open source stellar structure and evolution code (Paxton *et al.* 2011, 2013, 2015). It combines a series of numerical and physical models to calculate all astrophysical phenomena related to stars. It is composed of multiple modules and each module runs independently. MESA has been widely used in research by our group (Lü *et al.* 2013; Yan *et al.* 2016; Lü *et al.* 2017; Zhu *et al.* 2017). In this work, we use MESA to calculate the neutrino luminosity of stars with different masses at different stages of stellar evolution.

MESA can calculate the neutrinos produced by nuclear and thermal process. The nuclear reaction network used in this work is `o18_and_ne22.net` (Paxton *et al.* 2011), which has 10 elements,  $^1\text{H}$ ,  $^3\text{He}$ ,  $^4\text{He}$ ,  $^{12}\text{C}$ ,  $^{14}\text{N}$ ,  $^{16}\text{O}$ ,  $^{20}\text{Ne}$ ,  $^{24}\text{Mg}$ ,  $^{18}\text{O}$  and  $^{22}\text{Ne}$ . The nuclear reactions in the network are the PP chain, CNO cycle, He burning and some auxiliary reactions. In the PP chain, the nuclear reactions that produce neutrinos include  $^1\text{H}(^1\text{H}, e^+ + \nu)^2\text{H}$ ,  $^1\text{H}(e^- + ^1\text{H}, \nu)^2\text{H}$ ,  $^7\text{Be}(e^-, \nu)^7\text{Li}$ ,  $^8\text{B}(e^+, \nu)^8\text{Be}$  and  $^3\text{He}(^1\text{H}, e^+ + \nu)^4\text{He}$ . In the CNO cycle, the nuclear reactions include  $^{13}\text{N}(e^+, \nu)^{13}\text{C}$ ,  $^{15}\text{O}(e^+, \nu)^{15}\text{N}$  and  $^{17}\text{F}(e^+, \nu)^{17}\text{O}$ . Neutrinos are not produced in helium burning (the nuclear reactions that produce in helium burning include  $^{12}\text{C}(\alpha, ^1\text{H})^{15}\text{N}(^1\text{H}, \gamma)^{16}\text{O}$ ,  $^{14}\text{N} + 1.5\alpha = ^{20}\text{Ne}$ ,  $^{16}\text{O}(\alpha, ^1\text{H})^{19}\text{F}(^1\text{H}, \gamma)^{20}\text{Ne}$  and  $^{20}\text{Ne}(\alpha, ^1\text{H})^{23}\text{Na}(^1\text{H}, \gamma)^{24}\text{Mg}$ ) and other auxiliary reactions.

MESA uses the fitting formula from Itoh *et al.* (1996) to calculate the neutrinos produced by different processes: plasmon decay, pair annihilation, bremsstrahlung, and photo-neutrinos. The above four processes greatly depend on the temperature and the density. The pair annihilation is particularly important when the temperature reaches  $10^9$  K (see also Bhattacharyya 2006). When the temperature is less than  $4 \times 10^8$  K and the density is lower than  $10^5$  g cm $^{-3}$ , the photon-neutrino process is dominant. Plasmon decay can be in a leading position when the temperature is about  $10^7 - 10^8$  K and the density is about  $10^4 - 10^7$  g cm $^{-3}$ . Bremsstrahlung can efficiently produce neutrinos when the density is  $10^8 \sim 10^{10}$  g cm $^{-3}$ .

In our calculations, we take  $Z = 0.02$  as stellar metallicity. The thermonuclear reaction rates were provided by the JINA Reaclib (Rauscher & Thielemann 2000; Sakharuk *et al.* 2006; Cyburt *et al.* 2010). The heat released by reactions is deposited in plasma, which explains the energy loss of neutrinos under the weak interaction. Electron

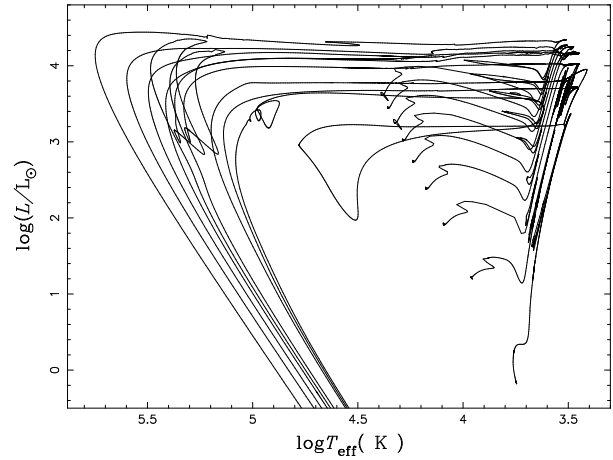


**Fig. 1** Evolutionary tracks for nine sequences in the Hertzsprung-Russell diagram. From bottom to top the stellar masses are 1, 2, 3, 4, 5, 6, 7, 8 and  $9 M_{\odot}$ .

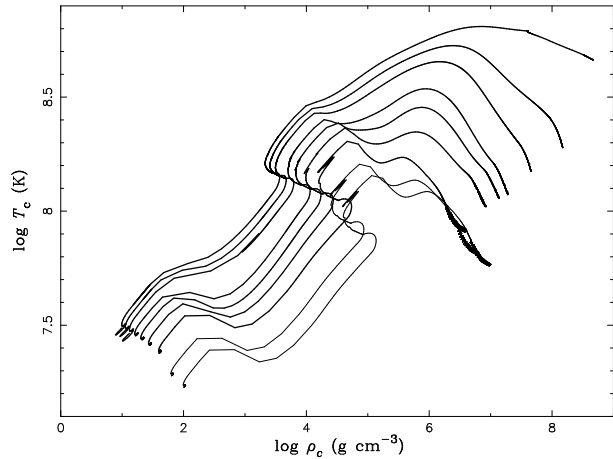


**Fig. 2** The evolution of central temperature and density for nine stars with different masses from the MS to the AGB stage. From bottom to top the stellar masses are 1, 2, 3, 4, 5, 6, 7, 8 and  $9 M_{\odot}$ .

screening factors extend the Graboske *et al.* (1973) methods using results from Alastuey & Jancovici (1978), along with plasma parameters from Itoh *et al.* (1979) for strong screening. We use Type 2 opacities (Iglesias & Rogers 1996) to increase the composition of C and O during helium burning (Paxton *et al.* 2011). Mixing length parameter ( $\alpha_{\text{MLT}}$ ) is taken as 1.73 (Cox & Giuli 1968). Due to the existence of composition gradients, the Ledoux criterion is considered in the convection model. Semiconvection and overshoot are widely used in MESA, both of which are time-dependent diffusion processes. In the mixing region, the semiconvection is unstable for Schwarzschild but stable for Ledoux (Langer *et al.* 1983). Here efficiency parameters for semiconvection ( $\alpha_{\text{sc}}$ ) and thermohaline mixing ( $\alpha_{\text{th}}$ ) are taken as 0.04 and 2.0, respectively. In the overshoot region, the overshoot mixing of exponential decay is used in all convective boundary regions, which is depicted

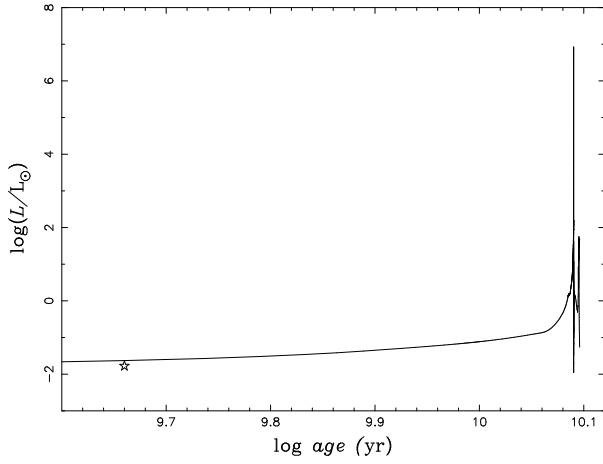


**Fig. 3** The neutrino-luminosity evolution of a star with  $1 M_{\odot}$  mass. The star symbol represents the solar neutrino luminosity observed. The observational data come from Bahcall (1997); McDonald (2004).

by Herwig (2000). We adopt  $f = 0.014$  and  $f_0 = 0.004$ . The mass-loss rates are taken from Reimers (1975) during the first giant branch (FGB) and from Bloeker (1995) on the asymptotic giant branch (AGB), respectively.

### 3 RESULTS AND DISCUSSION

Using MESA code, we calculate the evolutions of nine stars with masses of  $1\text{--}9 M_{\odot}$ . Stars in all models begin at Zero Age Main Sequence, and end as white dwarfs until  $\log L \approx -1.0$ . Figure 1 shows their evolutionary tracks on the Hertzsprung-Russell diagram. Based on Itoh et al. (1996), the four processes (plasmon decay, pair annihilation, bremsstrahlung, and photo-neutrinos) are greatly affected by the central temperature and the density. Figure 2 shows the evolution of central temperature and density for nine stars with different masses from the MS to the AGB stage.

#### 3.1 Standard Solar Model

Up till now, only solar neutrino flux has been measured, and it is about  $6.6 \times 10^{10} \text{ cm}^{-2} \text{ s}^{-1}$  on the Earth (e.g., Raffelt 2012). The relationship between solar neutrino flux and solar neutrino luminosity was given by Vissani (2018) to be

$$L_{\nu_e} = 4\pi D^2 \times \sum_i \langle E_i \rangle \phi_i, \quad (1)$$

where  $i$  represents the different nuclear reaction channels (including pp, pep, hep and  ${}^8B$ ), and the mean energies of neutrinos for these channels,  $\langle E_i \rangle$ , are equal to 0.265, 1.445, 9.628 and 6.735 MeV, respectively. Here,  $4\pi D^2 = 4.50579 \times 10^{21} \text{ erg cm}^2 \text{ MeV}^{-1}$ , and  $\phi(\text{pp}) = 6.5 \times 10^{10} \text{ cm}^{-2} \text{ s}^{-1}$ ,  $\phi(\text{pep}) = 1.61 \times 10^8 \text{ cm}^{-2} \text{ s}^{-1}$ ,

$\phi(\text{hep}) = 1.4 \times 10^3 \text{ cm}^{-2} \text{ s}^{-1}$  and  $\phi({}^8B) = 2.35 \times 10^6 \text{ cm}^{-2} \text{ s}^{-1}$  (Bahcall 1997; McDonald 2004). According to Equation (1), we calculate the current neutrino luminosity of the Sun. It is about  $0.02 L_{\odot}$ , which is marked by a star symbol in Figure 3. Simultaneously, Figure 3 also shows the evolution of neutrino luminosity with a standard solar model computed by MESA. MESA can provide physical quantities, such as temperature, density and the neutrino energy loss rates at any time of stellar evolution. It combines a series of physical quantities provided by its internal physical module to calculate and fit the neutrino luminosity. In order to verify the correctness of our model, we compared the neutrino luminosity obtained from observations and our simulation. We found that the value estimated by observation is basically consistent with that calculated by our model at  $4.61 \times 10^9 \text{ yr}$ .

Figure 4 shows the neutrino and the photo luminosities for the  $1 M_{\odot}$  model at the different evolutionary stages: the main sequence (MS), the first giant branch (FGB), the core helium burning (CHeB) and the asymptotic giant branch (AGB).

Panel (a) of Figure 4 shows a comparison of neutrino luminosity and photo luminosity for the MS stage. At these times, hydrogen fusion occurs in the stellar core. Based on the core temperature ( $\sim 1.5 \times 10^7 \text{ K}$ ), the neutrinos mainly originate from the PP chain. Compared with the photo luminosity, neutrino luminosity is very small. The energy carried away by neutrinos accounts for several percent of the total energy. Similar results can be found at the FGB stage, which is shown in panel (b). At that time, the hydrogen shell burning provides neutrinos.

Panel (c) of Figure 4 shows the neutrino luminosity at the CHeB stage. During this stage, helium burning does not produce neutrinos, but the thermal process can do. The central temperature and density are about  $10^8 \text{ K}$  and  $10^6 \text{ g cm}^{-3}$ , respectively. Based on Itoh et al. (1996), the neutrinos mainly originate from plasma decay. Because of a very small scatter cross section, the neutrinos take away a lot of energy from the core. Meanwhile, the helium core is partially degenerate and the helium burning leads to thermonuclear runaway. This corresponds to the helium burning peak which occurs simultaneously with the neutrino peak in Figure 4(c). In the helium flash phase, the neutrino luminosity is mainly provided by the thermal processes. After the helium flash, the electron degeneracy of the helium core is eliminated and the central helium burning is carried out in a smooth manner. At this time, neutrinos are not produced by helium burning but mainly originated from the hydrogen shell burning. In short, during the CHeB phase, the photons are mainly provided by helium burn-

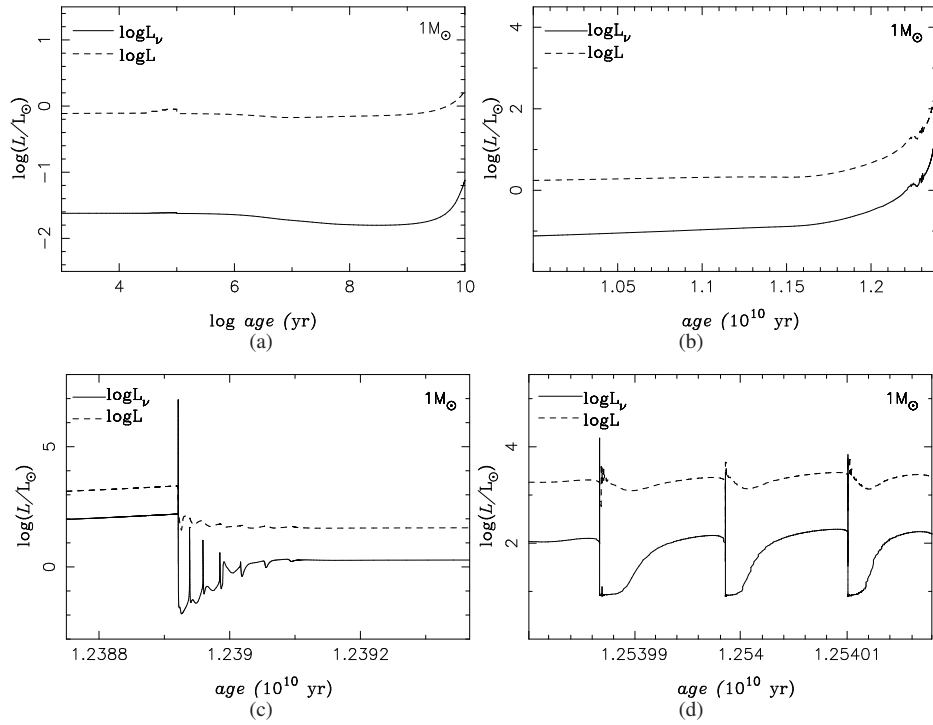


**Fig. 4** The neutrino and the photo luminosities for the  $1 M_{\odot}$  model at the different evolutionary stages. The *solid lines* represent the neutrino luminosity, and the *dashed lines* the photo luminosity. The main sequence, first giant branch, core helium burning and asymptotic giant branch stages correspond to (a), (b), (c) and (d), respectively.

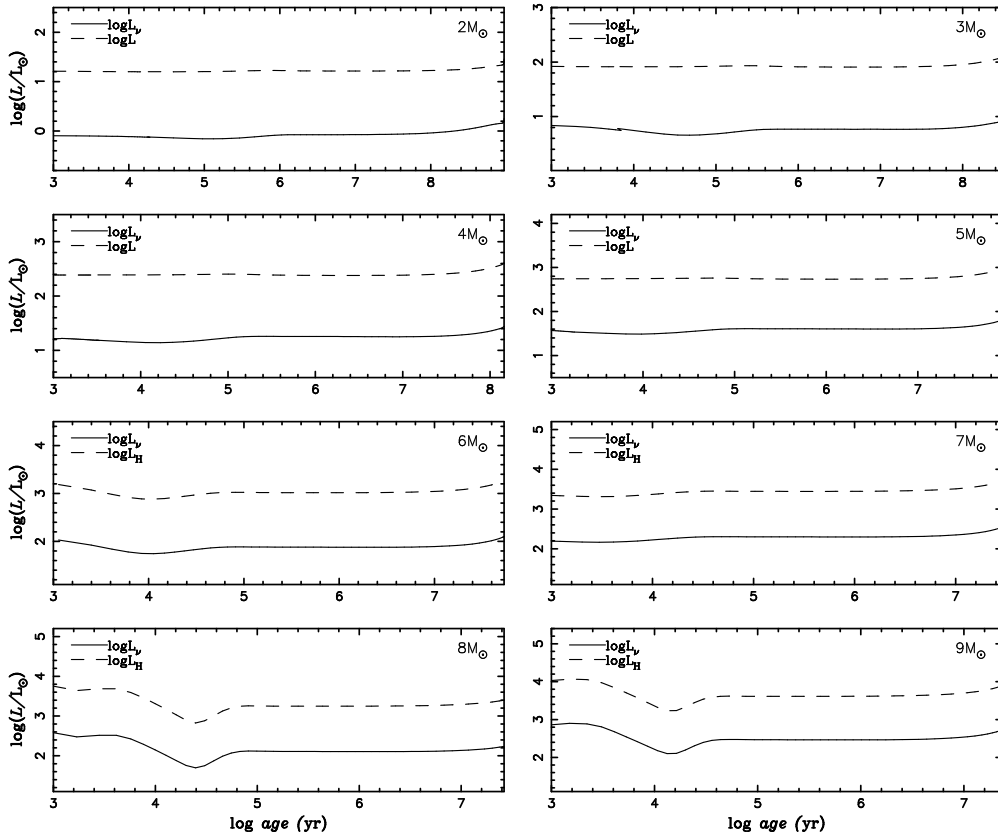


**Fig. 5** The photo and neutrino luminosities for stellar models with different masses at the MS stage. The *solid lines* represent the neutrino luminosity, and the *dashed lines* the photo luminosity. The stellar masses are plotted in the top-right zone in each panel.

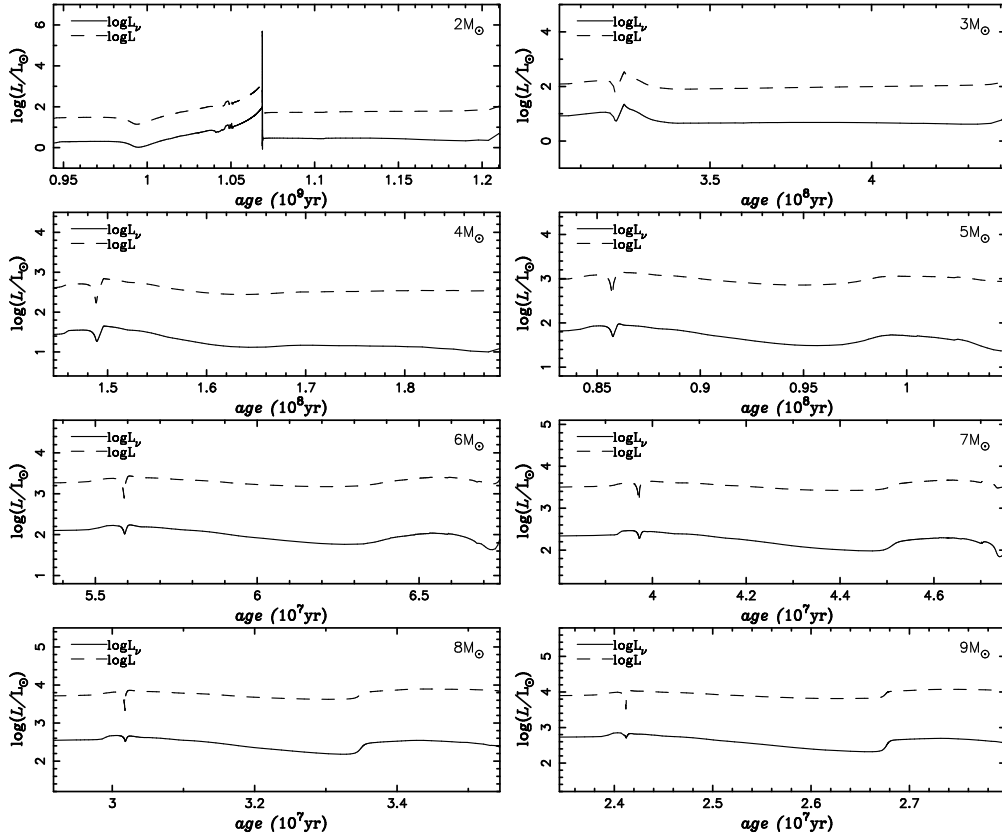


Fig. 6 Similar to Fig. 5, but for the FGB and CHeB stages.

ing, while the neutrinos mainly come from hydrogen shell burning except for the helium flash phase during which the thermal process – plasma decay – produces most of the neutrinos.

Panel (d) of Figure 4 shows the neutrino luminosity at the AGB stage. At this time, helium shell burning is carried out in an explosive manner (also called helium shell flash), which is similar to the central helium burning in the degenerate region. It releases a large amount of energy in a very short time. The thermal pulsation causes helium shell expansion and hydrogen shell cooling. Helium shell burning is similar to central helium burning. The nuclear reactions that occur in the helium shell burning do not produce neutrinos. Neutrinos are produced mainly in the thermal processes. The central temperature and density are about  $10^8$  K and  $10^6$  g cm $^{-3}$ , respectively. Therefore, the neutrinos mainly originate from plasma decay. Simultaneously, the helium shell burning is also accompanied by the emission of photons. Compared with the neutrino luminosity, the photon luminosity dominates except for at the helium shell flash stage, as shown in panel (d) of Figure 4. Comparing panels (c) and (d) of Figure 4, we find that the neutrino luminosity in the helium flash stage is larger than in the other stages. The reason is that the helium flash is a

thermonuclear explosion caused by degenerate electrons, and its neutrino luminosity is obviously affected by the electron degeneracy (Landstreet 1967).

### 3.2 Neutrino Luminosity of Stars with Different Masses at Different Evolution Stages

Except for the  $1 M_{\odot}$  star, we also study the evolutions of eight stars with masses of 2, 3, 4, 5, 6, 7, 8 and  $9 M_{\odot}$ . Figure 5 shows their photo and neutrino luminosities at the MS stage. Similarly to the  $1 M_{\odot}$  star, neutrinos are mainly supplied by the central hydrogen burning of the CNO cycle because the core temperatures of these stars are higher than  $2.0 \times 10^7$  K (see Fig. 2). Compared with the photo luminosities, the neutrino luminosities of these stars at the MS stages are very small. Of course, the more massive star is, the stronger the nuclear reaction is, and therefore, their neutrino luminosity is higher.

Considering that the timescale of the FGB is very short, we show the photo and neutrino luminosities at the FGB and CHeB phases for these stars in Figure 6. During the FGB stage, the neutrinos originate from hydrogen shell burning. During the CHeB stage, there is a peak in the neutrino luminosity of star with a mass of  $2 M_{\odot}$ . The main reason is similar to that for the  $1 M_{\odot}$  star, that is, he-

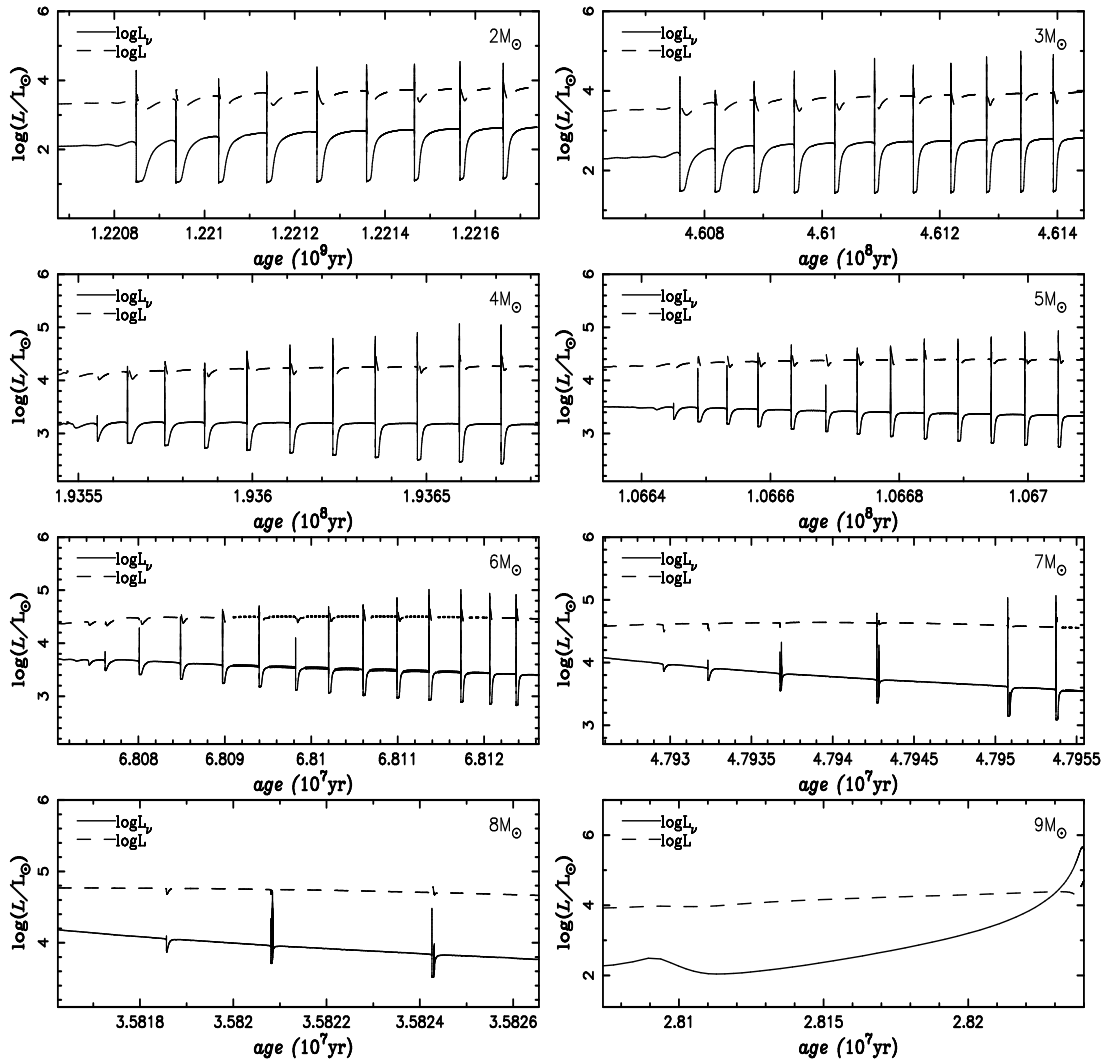
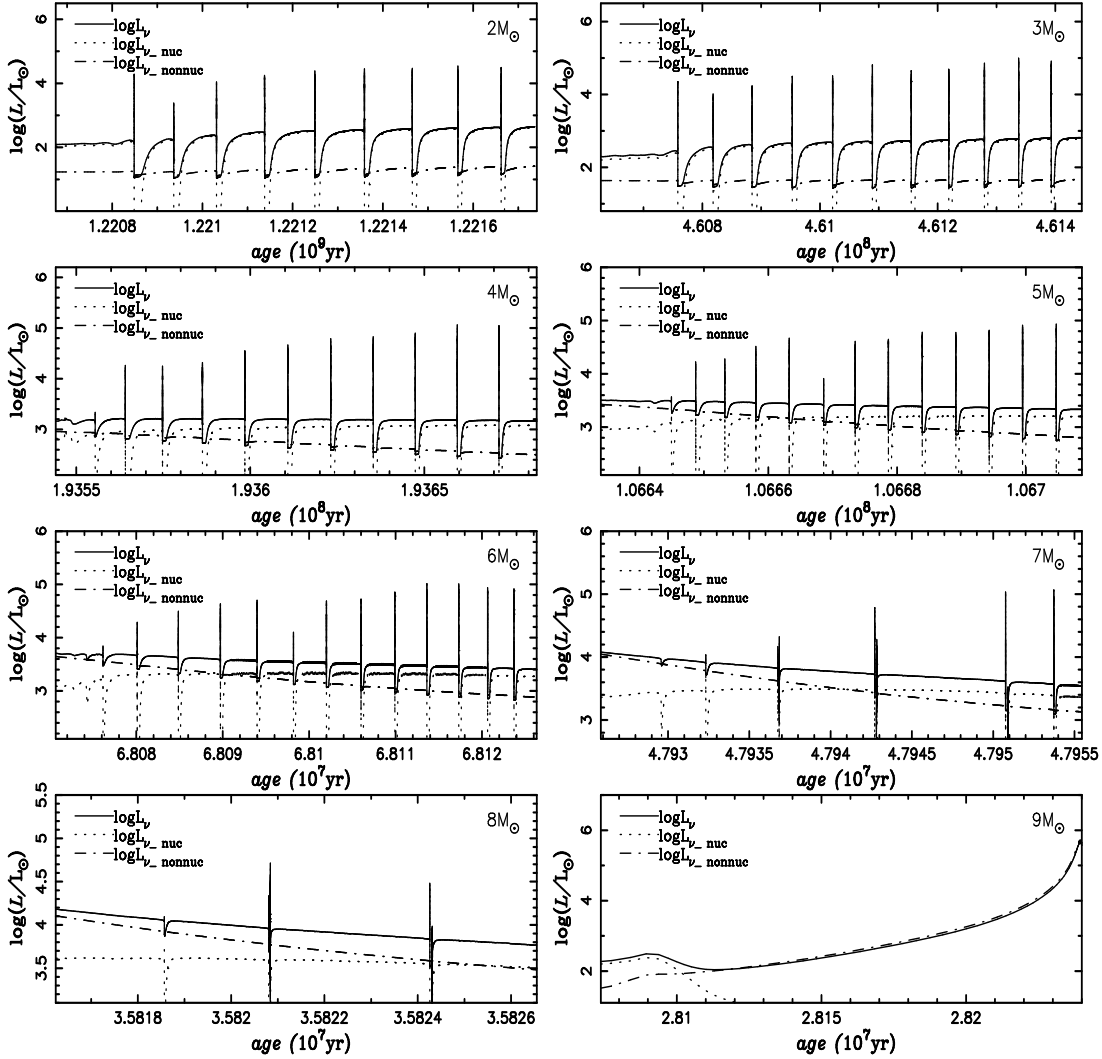


Fig. 7 Similar to Fig. 5, but for the AGB stage.

lium flash. The neutrino luminosity at the peak mainly results from thermal processes. At this time, as shown in Figure 2, because the central temperature and density are about  $10^8$  K and  $10^6$  g cm $^{-3}$ , respectively, the neutrinos mainly originate from plasma decay. However, the stars with masses larger than  $3 M_{\odot}$  have non-degenerate helium after the FGB stage. Their helium ignition process is relatively quiet, and the helium flash does not occur. Because helium burning does not produce neutrinos, the neutrinos are mainly produced by hydrogen shell burning around the helium core. Therefore, the neutrino luminosity is mainly from nuclear processes, and the contribution of thermal processes is very small.

Figure 7 shows the neutrino luminosity for the models of different masses at the AGB stages. In our simulations, the stars with masses between  $2$  and  $8 M_{\odot}$  undergo thermal-pulses triggered by helium flashes, which are similar to those of the  $1 M_{\odot}$  star. During the helium

flash, as shown in Figure 2, the central temperature is about  $10^8 \sim 10^{8.3}$  K, and the central density is about  $10^6 \sim 10^{7.6}$  g cm $^{-3}$ . Therefore, the neutrinos also mainly originate from plasma decay. During these helium flashes, the neutrino luminosity greatly increases. However, stars with  $9 M_{\odot}$  quickly lose their envelopes due to the high mass-loss rate when they enter the AGB stage. The thermal pulsation hardly occurs. In the final stage of stellar evolution, the stellar evolution is driven by gravitational energy release and thermal energy. Due to the decrease of ion pressure, the stellar core contracts and the gravitational energy is released. At that time, the neutrino luminosity is mainly provided by thermal processes, as we can see in Figure 8. The central temperature and the central density are about  $10^{8.2} \sim 10^{8.5}$  K and  $10^4 \sim 10^8$  g cm $^{-3}$ , respectively (see Fig. 2). Based on Itoh *et al.* (1996), the neutrinos mainly originate from plasma decay.



**Fig. 8** The neutrino luminosity produced by nuclear reactions and thermal processes at the AGB stages. The *solid*, *dotted* and *dot-dashed* lines represent the total neutrino luminosity, the neutrino luminosity produced by nuclear reactions and the neutrino luminosity produced by the thermal processes, respectively.

Figure 8 shows the neutrino luminosity produced by nuclear reactions and thermal processes at the AGB stage. We can see that the neutrino luminosity of stars with masses less than  $8 M_{\odot}$  is mainly derived from nuclear reactions, except for the helium flash stage at which neutrinos are derived from plasma decay. For the star with a mass of  $9 M_{\odot}$ , the neutrino luminosity originates from nuclear reactions until the end of the AGB stage. At the end of the AGB stage, the neutrino luminosity results from the plasma decay triggered by the gravitational energy release due to the contraction of the stellar core.

#### 4 CONCLUSIONS

In this work, we calculate the neutrino luminosity of stars with masses from 1 to  $9 M_{\odot}$  from the MS to AGB stages. Our result for the star with  $1 M_{\odot}$  mass at an evolution-

ary age of  $4.61 \times 10^9$  yr is consistent with the solar neutrino luminosity. In general, the neutrinos are produced by nuclear reactions, and the neutrino luminosity of stars is about one or two magnitudes lower than the photo luminosity. However, the neutrino luminosity can exceed the photo luminosity during the helium flash which can occur for stars with a mass lower than  $8 M_{\odot}$ . Although the helium flash does not produce neutrinos, plasma decay, one of the thermal processes, can efficiently make neutrinos during this stage. Due to the high mass-loss rate, the star with a mass of  $9 M_{\odot}$  does not undergo the helium flash. Its neutrinos mainly originate from nuclear reactions until the end of the AGB stage. At the end of the AGB stage, its neutrino luminosity results from thermal processes – the plasma decay which is triggered by the gravitational energy release because of the stellar core contracting.

**Acknowledgements** This work received the generous support of the National Natural Science Foundation of China (Grant Nos. 11763007, 11473024, 11463005, 11863005, 11803026 and 11503008). We would also like to express our gratitude to the Tianshan Youth Project of Xinjiang (2017Q014).

## References

- Alastuey, A., & Jancovici, B. 1978, *ApJ*, 226, 1034
- Bahcall, J. N., & Ulrich, R. K. 1988, *Reviews of Modern Physics*, 60, 297
- Bahcall, J. N. 1997, *Phys. Rev. C*, 56, 3391
- Bahcall, J. N., Krastev, P. I., & Smirnov, A. Y. 2001, *Journal of High Energy Physics*, 5, 015
- Bhattacharyya, I. 2006, *Journal of Physics G: Nuclear and Particle Physics*, 32, 2167
- Bionta, R. M., Blewitt, G., Bratton, C. B., et al. 1987, in *Neutrino Masses and Neutrino Astrophysics (Including Supernova 1987a)*, eds. V. Barger, F. Halzen, M. Marshak, & K. Olive, 63
- Bloecker, T. 1995, *A&A*, 297, 727
- Cox, J. P., & Giuli, R. T. 1968, *Principles of Stellar Structure* (New York: Gordon and Breach)
- Cyburt, R. H., Amthor, A. M., Ferguson, R., et al. 2010, *ApJS*, 189, 240
- Gamow, G., & Schoenberg, M. 1941, *Physical Review*, 59, 539
- Graboske, H. C., Dewitt, H. E., Grossman, A. S., & Cooper, M. S. 1973, *ApJ*, 181, 457
- Herwig, F. 2000, *A&A*, 360, 952
- Hirata, K., Kajita, T., Koshiba, M., et al. 1987, in *Neutrino Masses and Neutrino Astrophysics (Including Supernova 1987a)*, eds. V. Barger, F. Halzen, M. Marshak, & K. Olive, 51
- IceCube Collaboration, Aartsen, M. G., Ackermann, M., et al. 2018, *Science*, 361, 147
- Iglesias, C. A., & Rogers, F. J. 1996, *ApJ*, 464, 943
- Itoh, N., Totsuji, H., Ichimaru, S., & Dewitt, H. E. 1979, *ApJ*, 234, 1079
- Itoh, N., & Kohyama, Y. 1983, *ApJ*, 275, 858
- Itoh, N., Hayashi, H., Nishikawa, A., & Kohyama, Y. 1996, *ApJS*, 102, 411
- Keil, M. T., Raffelt, G. G., & Janka, H. T. 2003, *Nuclear Physics B Proceedings Supplements*, 118, 506
- Kohyama, Y., Itoh, N., Obama, A., & Mutoh, H. 1993, *ApJ*, 415, 267
- Landstreet, J. D. 1967, *Physical Review*, 153, 1372
- Langer, N., Fricke, K. J., & Sugimoto, D. 1983, *A&A*, 126, 207
- Lü, G., Zhu, C., & Podsiadlowski, P. 2013, *ApJ*, 768, 193
- Lü, G., Zhu, C., Wang, Z., & Imminiyaz, H. 2017, *ApJ*, 847, 62
- Masevich, A. G., Kotok, É. V., Dluzhnevskaya, O. B., & Mazani, A. 1965, *Soviet Ast.*, 9, 263
- McDonald, A. B. 2004, *New Journal of Physics*, 6, 121
- Paxton, B., Bildsten, L., Dotter, A., et al. 2011, *ApJS*, 192, 3
- Paxton, B., Cantiello, M., Arras, P., et al. 2013, *ApJS*, 208, 4
- Paxton, B., Marchant, P., Schwab, J., et al. 2015, *ApJS*, 220, 15
- Raffelt, G. 2012, arXiv:1201.1637
- Rauscher, T., & Thielemann, F.-K. 2000, *Atomic Data and Nuclear Data Tables*, 75, 1
- Reimers, D. 1975, *Circumstellar Envelopes and Mass Loss of Red Giant Stars*, eds. B. Baschek, W. H. Kegel, & G. Traving, *Problems in Stellar Atmospheres and Envelopes* (New York: Springer-Verlag New York), 229
- Sakharuk, A., Elliot, T., Fisker, J. L., et al. 2006, in *American Institute of Physics Conference Series*, 819, *Capture Gamma-Ray Spectroscopy and Related Topics*, eds. A. Woehr, & A. Aprahamian, 118
- Sukhbold, T., Ertl, T., Woosley, S. E., Brown, J. M., & Janka, H. T. 2016, *ApJ*, 821, 38
- Vissani, F. 2018, arXiv:1808.01495
- Yan, J.-Z., Zhu, C.-H., Wang, Z.-J., & Lü, G.-L. 2016, *RAA (Research in Astronomy and Astrophysics)*, 16, 141
- Zhu, C., Lü, G., & Wang, Z. 2017, *ApJ*, 835, 249